이학박사 학위논문

NAD 치료의 항비만 효과의 시상하부 기전 연구

Hypothalamic mechanisms of anti-obesity effect of nicotinamide adenine dinucleotide treatment

2018 년 2 월

울산대학교 대학원

의 학 과

노 은

Doctor of Philosophy

Hypothalamic mechanisms of anti-obesity effect of nicotinamide adenine dinucleotide treatment

NAD 치료의 항비만 효과의 시상하부 기전 연구

February 2018

The Graduate School of the University of Ulsan

Department of Medicine

Roh, Eun

Hypothalamic mechanisms of anti-obesity effect of nicotinamide adenine dinucleotide treatment

지 도 교 수　　김 민 선

이 논문을 이학박사 학위 논문으로 제출함

2018 년　02 월

울산대학교 대학원

의 학 과

노 은

노은의 이학박사학위 논문을 인준함

심사위원 송 영 섭 (인)

심사위원 김 민 선 (인)

심사위원 권 미 나 (인)

심사위원 고 은 희 (인)

심사위원 최 형 진 (인)

울산대학교 대학원

2018 년 02 월

Abstract

Nicotinamide adenine dinucleotide (NAD)-dependent deacetylase SIRT1 is an important regulator of hypothalamic neuronal function. Thus, adequate hypothalamic nicotinamide adenine dinucleotide (NAD) content has been reported to be critical for maintaining normal energy homeostasis and circadian rhythm. In mammalian cells, NAD is largely recycled via nicotinamide and nicotinamide mononucleotide (NMN). Previous studies have shown that supplementation with NMN improves obesity/ageing-related metabolic complications in rodents.

I investigated whether exogenous NAD increases hypothalamic neuron NAD levels and affects energy metabolism. I also explored mechanisms mediating central metabolic effects of NAD supplement.

I found that extracellular NAD was imported into N1 hypothalamic neuronal cells in a connexin 43-dependent manner. Exogenous NAD effectively suppressed NPY and AgRP transcriptional activity, and this effect was mediated by SIRT1 and FOXO1. In mice, central

and peripheral NAD administration suppressed fasting-induced hyperphagia and weight gain. Consistent with the *in vitro* data, inhibition of hypothalamic connexin 43 blocked hypothalamic neuronal NAD uptake as well as NAD-induced anorexia and weight reduction.

Diet-induced obese mice had lower hypothalamic NAD content compared to lean mice. Chronic NAD supplement in obese mice rescued hypothalamic NAD deficit and corrected blunted circadian rhythms in feeding, locomotor activity, and energy expenditure. These findings indicate that NAD supplementation is a potential therapeutic method for metabolic disorders accompanied by hypothalamic NAD depletion.

Key words: hypothalamus, obesity, energy homeostasis, circadian rhythm, connexin

Contents

List of figures

1. Introduction

Nicotinamide adenine dinucleotide (NAD) regulates the cellular redox state by mediating hydride transfer in oxidoreductive metabolic processes [1]. NAD is converted to NADH in glycolytic reaction catalyzed by glyceraldehyde 3-phosphate dehydrogenase and the four steps of the tricarboxylic acid (TCA) cycle [2]. NAD is also converted to NADH during the oxidation of fatty acids and amino acids in mitochondria. To maintain a proper redox state, NADH needs to be reoxidized, serving as an electron donor for oxidative phosphorylation and ATP synthesis [2].

Moreover, NAD is a pivotal cosubstrate in many biochemical reactions, which are catalyzed by the NAD-dependent deacetylase/ADP-ribosyltransferase sirtuins, poly(ADP-ribose) polymerase (PARP), and cyclic ADP-ribose cyclase/CD38 [3, 4]. NAD-dependent deacetylase sirtuins play important roles in cellular adaptive responses to stresses such as fasting, DNA damage, and oxidative stress [5]. A representative sirtuin SIRT1 is the mammalian orthologue of Sir2, which mediates caloric restriction-induced longevity in

yeasts [6]. In peripheral metabolic organs, SIRT1 controls cellular metabolism by deacetylating key transcriptional regulators including peroxisome proliferator-activated receptor-γ (PPARγ), PPARγ coactivator-1α (PGC-1α), and forkhead transcription factor FOXOs [7-9].

The classical Preiss-Handler pathwsay of NAD synthesis, which starts from nicotinic acid (NA), is predominant in unicellular organisms and requires subsequent amidation of the NA moiety by NAD synthetase [10]. In mammals, most cellular NAD is synthesized via a recycling pathway in which nicotinamide is converted to nicotinamide mononucleotide (NMN) by nicotinamide phosphoribosyltransferase (Nampt) and then to NAD by nicotinamide mononucleotide adenylyltransferase (Nmnat) [3, 4]. On the other hand, NAD can be *de novo*-synthesized from tryptophan or synthesized from nicotinamide ribose (NR), a trace nutrient in foods [3, 4]. In the latter NAD biosynthetic pathway, NR is converted to NMN by the NR kinase (NRK) and then to NAD by the Nmnat.

Recent studies have also demonstrated a critical role for SIRT1 in the hypothalamic regulation of energy balance and circadian physiology [11-15]. SIRT1 in the anorexigenic

proopiomelanocortin (POMC) neurons of hypothalamic arcuate nucleus (ARC) and SF1 neurons of ventromedial nucleus acts to counter diet-induced obesity [13, 16]. In contrast, SIRT1 in the orexigenic neuropeptide Y (NPY)/*Agouti*-related protein (AgRP) neurons is an important determinant of neuronal excitability and response to ghrelin [14]. Furthermore, SIRT1 in the master clock neurons of hypothalamic suprachiasmatic nucleus (SCN) interacts with two major circadian regulators, BMAL1 and CLOCK [17], to critically regulate the transcription of circadian clock genes [18, 19]. Notably, SIRT1 expression in the hypothalamic ARC and SCN decreases with aging [17, 20], and this phenomenon has been suggested as a central mechanism for age-associated weight gain and decline in circadian function [17, 20]. In addition to aging, chronic consumption of high-fat, high-sucrose diet also reduces hypothalamic SIRT1 protein levels and NAD content in mice, which leads to low SIRT1 activity in hypothalamic neurons [20].

Given the critical importance of NAD-dependent SIRT1 activity in normal metabolic functions [21], therapeutic strategies activating the cellular NAD-SIRT1 axis have been proposed. Several lines of evidences showed metabolic benefits of SIRT1-activating

compounds including polyphenols such as resveratrol and synthetic small molecule activators of SIRT1 [22-25]. The limitation of this strategy is that SIRT1 activity is dependent on cellular NAD contents. Therefore, there have been trials to increase NAD levels in metabolic organs by supplying NAD precursors [26-28], which have shown that supplementation with NAD precursors NMN and NR produce beneficial metabolic effects in obese or aged mice by restoring NAD levels in peripheral metabolic organs. However, these studies did not clearly show how exogenous NMN and NR enter cells to elevate cellular NAD levels. Interestingly, a recent study has shown that NMN is extracellularly converted to NR by the ecto-5'-nucleotidase (CD73), and that NR is subsequently imported into cells via equilibrative nucleoside transporters [29].

It has been previously shown that extracellular NAD treatment can increase cellular NAD levels and rescue cells from NAD depletion-induced death [30]. Therefore, I investigated the effect of exogenous NAD in increasing hypothalamic neuronal NAD contents, and attempted to identify the molecular mechanism of hypothalamic neuronal NAD uptake. I also examined the effects of centrally- and peripherally-administered NAD on

energy metabolism in lean and obese mice.

2. Materials and methods

2.1. Materials

NAD, carbenoloxolone (CBN), cytidine 5′-monophosphate (CMP), adenosine 5′-diphosphate (APCP), and sirtinol were purchased from Sigma-Aldrich (St. Louis, MO, USA). FK866 was obtained from Enzo Life Sciences (Farmingdale, NY, USA) and EX527 from Tocris (Bristol, UK). Fluorescein isothiocyanate- conjugated NAD (FITC-NAD) was obtained from Trevigen (Gaithersburg, MD, USA).

2.2. Cell culture

N1 hypothalamic neuron cells were maintained in DMEM supplemented with 10% fetal bovine serum and 5% penicillin/streptomycin. SHSY-5Y and AtT-20 cells were cultured in DMEM containing 10% fetal calf serum.

2.3. Animals

Male C57BL/6N mice were fed a standard chow diet (CD; 12.5% of calorie from fat; Cargill Agri Purina, Inc., #38057, Seongnam, Korea) ad libitum unless mentioned otherwise. Mice were housed under controlled temperature (22 ± 1 ℃) with 12 h light-dark cycle, with light from 8 a.m. to 8 p.m. Diet-induced obesity (DIO) mice were fed on a 60% high fat diet (HFD; 60% of calorie from fat; Research Diets Co., #D12492; New Brunswick, NJ) from 8 weeks of age for 8 weeks. All procedures were approved by the Institutional Animal Care and Use Committee of the Asan Institute for Life Sciences (Seoul, Korea).

2.4. Cellular NAD uptake

To determine cellular NAD uptake, N1 hypothalamic neuronal cells were plated in 100 mm dishes and grown to approximately 90% confluence. Cells were pretreated with CBN (1 μM), CMP (1 and 10 μM), APCP (1 and 10 μM), FK866 (10 nM) or vehicle (PBS or DMSO) for 1 h and then treated with NAD (10 nM) for 30 min. Cells were washed with PBS twice and then lysed using 100 μl of 1M $HClO_4$ and neutralized by adding 33 μl of 3M K_2CO_2. After centrifuging (4 °C, 13,000 g) for 15 min, 25 μl of supernatant was mixed with 175 μl of 50

mM K_2PO_4/$KHPO_4$ (pH 7.0) and 100 μl of the mixture was loaded onto the HLPC column (Apollo C18, 5 μm, 250 x 4.6 mm, Alltech, Deerfield, IL, USA). High performance liquid chromatography (HPLC) was run at a flow of 1 ml/min. NAD was eluted as a sharp peak at 11 min as described previously [31, 32].

2.5. FITC-NAD study

To visualize cellular FITC-NAD uptake, cells were pretreated with CBN (1 μM) or vehicle (PBS) for 1 h before FITC-NAD treatment. One hour after FITC-NAD treatment (250 nM), cells were washed with PBS three times to remove FITC-NAD in the medium. FITC fluorescence was examined by live cell imaging system using confocal microscopy (Leica, Wetzlar, Germany). In in vivo study, FITC-labeled NAD (250 pmol in 2 μl) was administered via ICV-implanted cannulae. One hour after injection, whole brain was obtained to examine hypothalamic uptake of FITC-NAD.

2.6. Promoter analysis

Promoter assay of human NPY, AgRP, and mouse POMC was performed using luciferase reporter constructs containing the NPY promoter (pGL3-hNPY-luc; nucleotides –963 to +67), the AGRP promoter (pGL3-hAGRP-luc; nucleotides –1000 to –1), the POMC promoter (pGL3-mPOMC-luc; nucleotides –2301 to +34) as described in our previous study [33]. Forty-eight hours after transfection, cells were treated with NAD with or without EX527 (200 nM), sirtinol (100 nM), and FK866 (10 nM) for 2 or 4 h. For period 1 (PER1) promoter analysis, N1 cells were transfected with pGL3-mPER1 promoter-luciferase construct (nucleotides –1,803 to +40) and/or plasmids expressing pcDNA3.1-mBMAL1 (GenBank accession number NM007489) and pcDNA3.1-mCLOCK (GenBank accession number NM007715), and β-galactosidase (50 ng each). To study the effect of clock genes on the NPY and AgRP promotor activity, cells were transfected with pGL3-hNPY-luc or pGL3-hAGRP-luc with or without plasmids expressing pSCT1-mPER1 (GenBank accession number NM011065), pSCT1-mPER2 (GenBank accession number NM011066), pcDNA3.1-mBMAL1, and pcDNA3.1-mCLOCK. Cells were lysed and extracted to measure luciferase activity by a luminometer (PerkinElmer, Monza, Italy) and normalized for β-galactosidase

activity.

2.7. Intracerebroventricular cannulation and injection

Intracerebroventricular cannulation and injection was performed as previously described [33]. Mice were implanted with permanent 26-gauge stainless steel cannulae into the 3rd ventricle (1.8 mm caudal to the bregma and 5.0 mm ventral to the sagittal sinus) using a stereotaxic surgery. After one week-recovery period, mice were handled daily for 1 week to minimize stress responses. Correct positioning of the cannulae was confirmed by positive dipsogenic responses to angiotensin II (50 ng). Only the mice with correctly positioned cannulae were included in the data analysis. NAD, CBN, and CMP were dissolved in normal saline whilst EX527 and sirtinol were dissolved in DMSO-saline before injection. All compounds were administered in a volume of 2 μl.

2.8. Feeding study

Mice (8–10 weeks-old males) were individually housed for 1 week before study

commencement to minimize stress. One day before study commencement, the animals were randomly assigned to groups based on their body weights in order to match the average body weight of each group. NAD with or without inhibitors were intracerebroventricularly (ICV) or intraperitoneally (IP) injected in the early light phase (9–10 a.m.) to overnight-fasted mice. Control mice received the same volume of vehicle. Food intake was monitored at 1, 2, 4, 8, and 24 h after injection. Body weight was measured before and 24 h post-injection. For chronic NAD treatment, NAD (1 mg/kg) was daily injected intraperitoneally at 1 h before light-off for 4 weeks. Body weight and food intake were daily monitored before NAD injection.

2.9. Conditioned taste aversion study

Mice were habituated to a daily 1-h period of access to water. During this hour, two bottles containing unflavored tap water were placed in each home cage. After seven days, all mice received two bottles containing 0.15% saccharin instead of water. Immediately following this 1-h period of saccharin exposure, the mice received sequential injections of saline (IP)-saline

(ICV), lithium chloride (LiCl, 200 mg/kg, IP; Sigma)-saline (ICV), or saline (IP)-NAD (0.7 ng, ICV). For the next three consecutive days, a two-bottle choice test was conducted; in this test, the mice were allowed 1-h access to one bottle of tap water and another bottle of 0.15% saccharin solution. Preference ratio was calculated as the intake of saccharin solution/total intake of water and saccharin solution.

2.10. Energy expenditure study

Energy expenditure was measured using a comprehensive lab monitoring system (CLAMS) (Columbus Instruments Inc., Columbus, OH, USA). Mice were placed in the CLAMS chambers for 48 h and fasted overnight before measurement. Either saline or NAD at the indicated doses was administered ICV or IP in the early light phase, and EE was monitored for four hours following NAD injection.

2.11. Monitoring of circadian behaviors

Circadian rhythm of food intake, energy expenditure, and locomotor activity were

determined by using CLAMS. For adaptation purpose, the animals were placed in the CLAMS cambers for 48 h before measurement. During the CLAMS study, animals did not receive NAD injections in order to keep the metabolic chambers closed. Light and dark cycles were kept the same as in the home cages.

2.12. Measurement of hypothalamic NAD contents

Mice fed on CD or HFD for 8 weeks with or without NAD supplement were sacrificed by decapitation following a 5 h fast and 20 h later from the last NAD injection. The mediobasal hypothalamus (MBH) was dissected with the lateral border of half way to lateral sulcus and upper border of half way to anterior commissure as previously described [34]. Hypothalamic blocks were snap frozen in liquid nitrogen, and stored at −70°C before assay. Hypothalami were weighed immediately after thawing, lysed in 150 μl of 1 M $HClO_4$, and the neutralized by adding 50 μl of 3 M K_2CO_2. Following centrifugation (4 °C, 13,000 g) for 15 min, 20 μl of supernatant was loaded onto the HLPC column as described above. The amounts of NAD were normalized by wet tissue weights as described previously (28,29).

2.13. Determination of mRNA expression

Mouse hypothalamic ARC was collected at 1 h post-ICV NAD injection using the micropunch technique that used a Harvard brain matrix and blunted 20 gauge-metal needles (inner dimeter 0.91 mm). Bilateral ARC was collected from two consecutive brain slices (1 mm thick). The thickness of brain slice was 1 mm. RNA was also obtained from N1 cell, mouse liver, and hypothalamus to compare the expression levels of CD73 and connexin 43 (Cx43). mRNA expression was determined by real-time PCR analysis (Life Technologies, Carlsbad, CA) using corresponding primers: NPY (5′-atgctaggtaacaagcgactggg-3′ and 5′-ggctggatctcttgccatatctc-3′), AgRP (5′-acaactgcagaccgagca-3′ and 5′-gacgcggagaacgagact-3′) [33], POMC (5′-caggtcctggagtccgac-3′ and 5′-catgaagccaccgtaacg-3′) [33], SIRT1 (5′-gttctgactggagctggggt-3′ and 5′-tctgggaggtctgggaagtc-3′), SIRT3 (5′-gcctgaagacagctccaaca-3′ and 5′-gacatccctggtcagccttt-3′), CD73 (5′-aacccctttcctctcaaatcca-3′and 5′-cagggcgatgatcttattcacat-3′) [35] and Cx43 (5′-acagcggttgagtcagcttg-3 and 5′-gagagatggggaaggacttgt-3′) [36]. PCR primer sequences of NPY, SIRT1, and SIRT3 were

retrieved from the online PrimerBank database. Expression of each mRNA was normalized to that of glyceraldehyde-3-phosphate dehydrogenase (GAPDH). For presenting quantitative real-time PCR data, comparative C_T method was used.

2.14. siRNA studies

Small interfering RNA (siRNA) specific to murine Cx43 was purchased from Dharmacon (Chicago, IL, USA). Under anesthesia, Cx43 siRNA (0.5 nmol in 500 nl/each injection site) was microinjected bilaterally into the ARC. Nighttime food intake was measured on the second day after siRNA injection following ICV injection of saline or NAD (0.7 ng for ICV or 1 mg/kg for IP study) 1 h before light-off. In the morning of the 3rd post-injection day, mice were sacrificed to collect hypothalamic block or whole brain 1 h after ICV or IP injection of NAD ICV injection of FITC-NAD (650 ng). Knockdown was considered successful if MBH Cx43 mRNA or protein expression was decreased by more than 50% of the average Cx43 expression of controls. Successful knockdown was achieved in about 60% of mice treated with Cx43 siRNA. Only the animals with successful knockdown were

included in data analysis. An equal amount of non-targeting, scrambled control siRNA (Dharmacon) was administered to the control group. To deplete Cx43 expression in the N1 cells, cells were transfected with Cx43 siRNA (160 pmol/6 well).

2.15. Immunohistochemistry

Mice were perfused with 50 ml saline followed by 50 ml 4% paraformaldehyde via the left ventricle. Whole brains were collected, fixed with 4% paraformaldehyde for 24 h, and dehydrated in 30% sucrose solution until brains sank to the bottom of the container. I obtained coronal brain slices (25 μm thick) using cryostat (Leica, Wetzlar, Germany) and pre-mounted on charged glass slides (MUTO Pure Chemicals Co., Tokyo, Japan) for immunohistochemistry. Hypothalamic slices (25 μm thick) were permeabilized in 0.5% PBST for 5 min and blocked with 3% BSA at room temperature for 1 h and for anti-Cx43 antibody (rabbit, 1:1000, Abcam, Cambridge, UK) at 4°C overnight. After washing, slides were incubated with the Alexa-Flour 555-conjugated secondary antibodies (1:1000, Invitrogen, Carlsbad, CA) at room temperature for 1 h.

2.16. Statistical analysis

Data are presented as means ± SEM. Statistical analysis was performed using SPSS software version 22.0 (SPSS, Chicago, IL, USA). Statistical significance among the groups was tested with one-way ANOVA followed by a post hoc Fishers Least Significant Difference test, or an unpaired Student's t-test when appropriate. Repeated measures ANOVA was used to analyze the effect of chronic NAD supplement on body weight changes. Significance was defined as $P < 0.05$.

3. Results

3.1. Hypothalamic neurons uptake NAD through gap junction protein connexin 43

I firstly tested if exogenous NAD can affect cellular NAD levels in N1 hypothalamic neuronal cells. Treatment of N1 cells with a specific NAMPT inhibitor, FK866 (10 nM for 2 h) reduced intracellular NAD contents by ~25%, and this drop was rescued by extracellular application of NAD (10 nM for 30 min) (Figure 1), suggesting that extracellular NAD may enter cells to replenish the cellular NAD content. Intercellular gap junctions, especially Cx43 hemichannels, have been shown to mediate transmembrane NAD trafficking in 3T3 fibroblasts [37]. Notably, higher expression of Cx43 was found in the hypothalamus than in the liver of normal mice (Figure 2). Moreover, when N1 cells were pre-treated with gap junction inhibitor CBN, exogenous NAD-induced increase in cellular NAD levels were significantly blunted (Figure 3A). Consistently, siRNA-mediated Cx43 knockdown

prevented the exogenous NAD treatment-induced elevation of cellular NAD levels (Figure 3B), indicating an involvement of gap junctional protein, especially Cx43 in NAD influx to hypothalamic neurons.

A recent paper has suggested the possibility that NAD is extracellularly degraded to NMN and then to NR by the CD73 ecto-5'-nucleotidase [38], which is then transported into cells via the nucleoside transporters. To test this possibility, I co-treated N1 cells with exogenous NAD treatment and CD73 inhibitors CMP or APCP. In contrast to gap junction inhibitor, treatment of CD73 inhibitors failed to block an increase in cellular NAD levels following exogenous NAD (Figure 4A and B). Moreover, CD73 expression was lower in the hypothalamus compared to the liver (Figure 2), suggesting that CD73 might have a relatively minor role in NAD metabolism in the hypothalamus.

In order to directly visualize cellular uptake of NAD, I treated N1 cells with FITC labeled-NAD (250 nM) in the presence or absence of CBN. In FITC-NAD, FITC is attached to adenine residue of NAD (Figure 5); therefore, FITC signal is not detected inside cells if NAD is converted to NMN and NR before cellular uptake. Indeed, FITC signal was found in

the cytosolic compartment of N1 cells 1 h after treatment which was significantly reduced by co-treatment of CBN (Figure 6). These results support the notion of gap junction-mediated NAD uptake in hypothalamic neuronal cells.

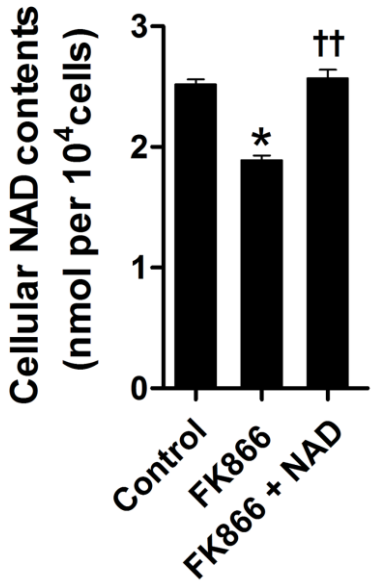

Figure 1. Extracellular NAD replenish cellular NAD depletion induced by FK866. N1 hypothalamic neuronal cells were treated with FK866 (10 nM) with or without NAD (10 nM). Cellular NAD contents were measured using HPLC. Results are presented as mean ± SEM. *$P < 0.05$ vs. control. $^{\dagger\dagger}P < 0.01$ vs. FK866 alone.

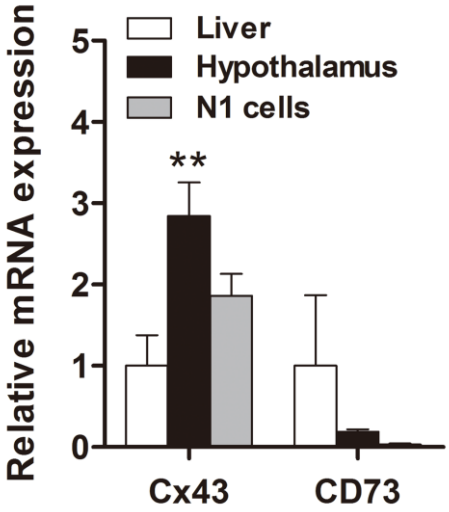

Figure 2. The mRNA expression of Cx43 and CD73 in the young mouse liver/hypothalamus and N1 cells. RNA was also obtained from N1 cell, mouse liver, and hypothalamus to compare the expression levels of CD73 and Cx43. mRNA expression was determined by real-time PCR analysis. Expression of each mRNA was normalized to that of GAPDH. Results are presented as mean ± SEM. $^{**}P < 0.01$ vs. liver.

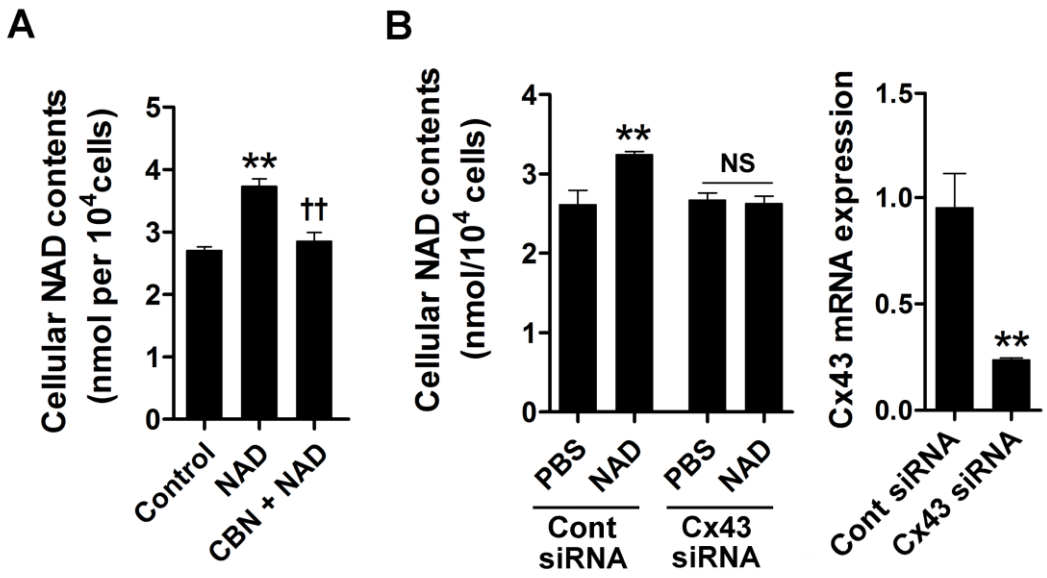

Figure 3. Blockade of NAD-induced increase in cellular NAD contents by connexin inhibitor CBN or Cx43 siRNA. (A and B) Cellular NAD levels were measured using HPLC after treatment of NAD (10 nM) with (A) pretreatment with gap junction inhibitor CBN (1 μM) or (B) siRNA-mediated Cx43 knockdown. N1 cells were pretreated with CBN or vehicle (PBS) for 1 h and then treated with NAD (10 nM) for 30 min. To deplete Cx43 expression in the N1 cells, cells were transfected with Cx43 siRNA (160 pmol/6 well). An equal amount of non-targeting, scrambled control siRNA was administered to the control group. Cx43 siRNA treatment significantly reduced cellular Cx43 expression. Results are presented as mean ± SEM. $^{**}P < 0.01$ vs. control, $^{\dagger\dagger}P < 0.01$ vs. NAD. NS: not significant.

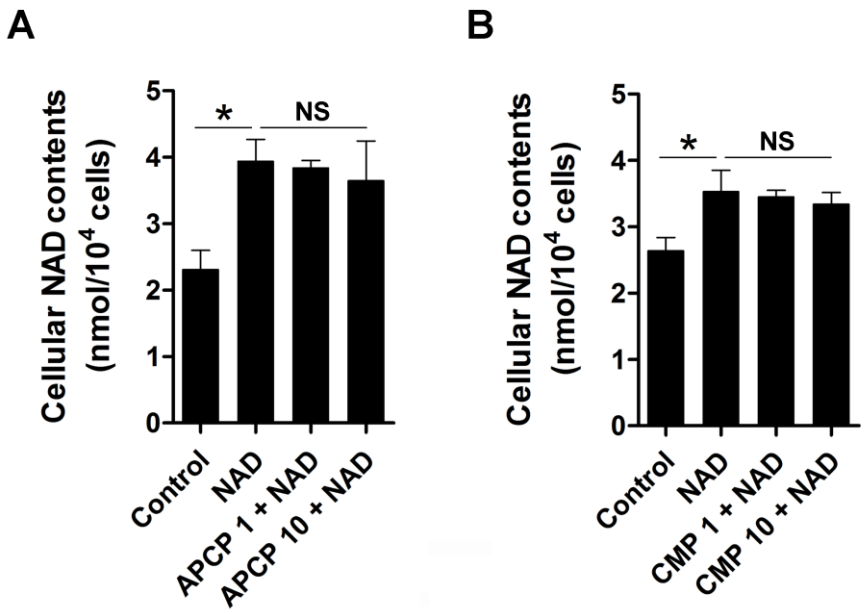

Figure 4. Effects of NAD alone or with CD73 inhibitors APCP and CMP on N1 cell NAD contents. (A and B) Cellular NAD contents after cotreatment with exogenous NAD and CD73 inhibitors (A) APCP or (B) CMP. To determine cellular NAD uptake, N1 cells were pretreated with CMP (1 and 10 μM), APCP (1 and 10 μM) or vehicle (PBS or DMSO) for 1 h and then treated with NAD (10 nM) for 30 min. Cellular NAD contents were measured using HPLC. Results are presented as mean ± SEM. **P* < 0.05 vs. control. NS: not significant.

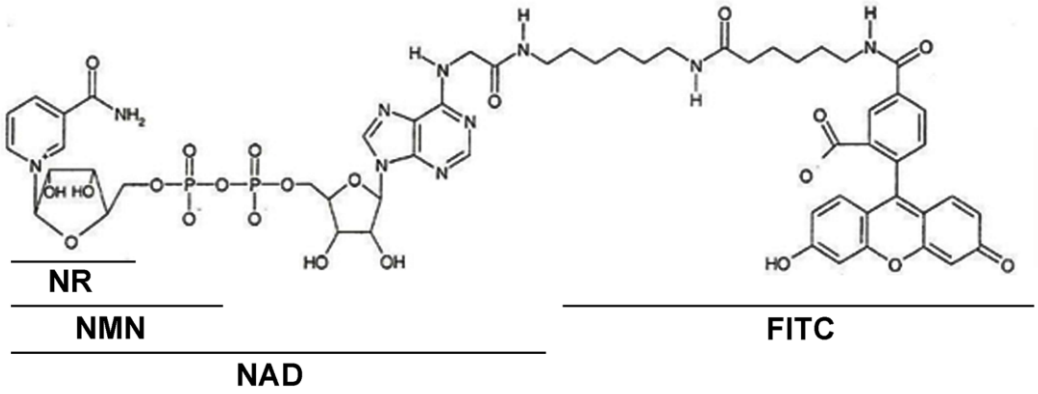

Figure 5. Molecular structure of FITC-NAD. NR: nicotinamide ribose, NMN: nicotinamide mononucleotide.

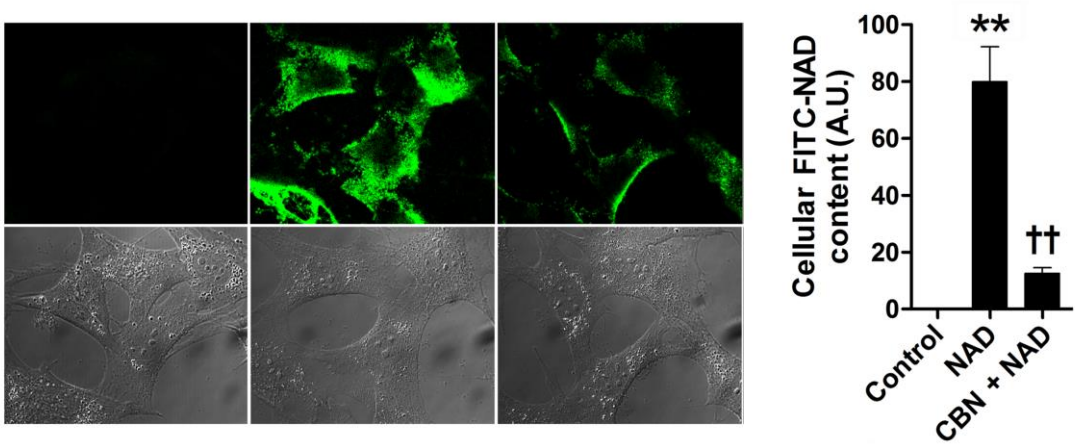

Figure 6. Cellular uptake of FITC-NAD in N1 cells in the absence or presence of CBN . To visualize cellular FITC-NAD uptake, cells were pretreated with CBN (1 μM) or vehicle (PBS) for 1 h before FITC-NAD treatment. FITC fluorescence was examined by live cell imaging system using confocal microscopy 1 h after FITC-NAD treatment (250 nM). $^{**}P < 0.01$ vs. control, $^{\dagger\dagger}P < 0.01$ vs. NAD.

3.2. Central and peripheral administration of NAD regulates energy metabolism

I next investigated if central administration of NAD may affect the food intake, body weight, and energy expenditure. Young C57 mice were injected with NAD (0.14, 0.7, and 1.4 ng) via ICV cannulae following an overnight fast. The doses of NAD were determined from the preliminary study in which I tested a wide range of doses (Figure 7A and B). Notably, injection of NAD (0.7 ng) significantly suppressed fast-induced feeding and weight gain compared to saline-injection (Figure 8A and B). The anorexigenic effect of NAD persisted for 24 h. To eliminate the possibility that NAD-induced anorexia and weight loss may be due to toxicity and systemic illness, I conducted a conditioned taste aversion (CTA) test. ICV injection of NAD (0.7 ng) did not affect saccharin preference, while intraperitoneal injection of lithium chloride, a well-known CTA inducer, significantly decreased saccharin consumption (Figure 9). Therefore, the effect of centrally-administered NAD is not likely to have been due to sickness or illness caused by the agent.

I also examined the effects of ICV-injected NAD on energy expenditure (EE), an important determinant of energy balance. For this, NAD (0.7 ng) was ICV-administered to freely-fed mice in the early light phase. EE was monitored for 4 h after ICV injections under food-deprived condition to avoid any possible effects of feeding on EE. EE significantly increased during the 2~4 h period post-NAD injection (Figure 10). I then investigated the effects of peripheral administration of NAD on energy metabolism, because administration of drugs or chemicals via peripheral routes is more applicable for therapeutic intervention in humans. For this purpose, normal mice were fasted overnight and injected with NAD (0.3, 1, and 3 mg/kg) intraperitoneally in the early light phase. IP injection of NAD (1 and 3 mg/kg) significantly decreased 4 h-food intakes (Figure 11). The anorectic effect of IP NAD (1 mg/kg) persisted at 24 h post-injection. In addition, EE significantly increased during the 2 - 4 h post-IP administration of NAD (1 mg/kg) and tended to increase during the 4 - 8 h post-injection period (Figure 12).

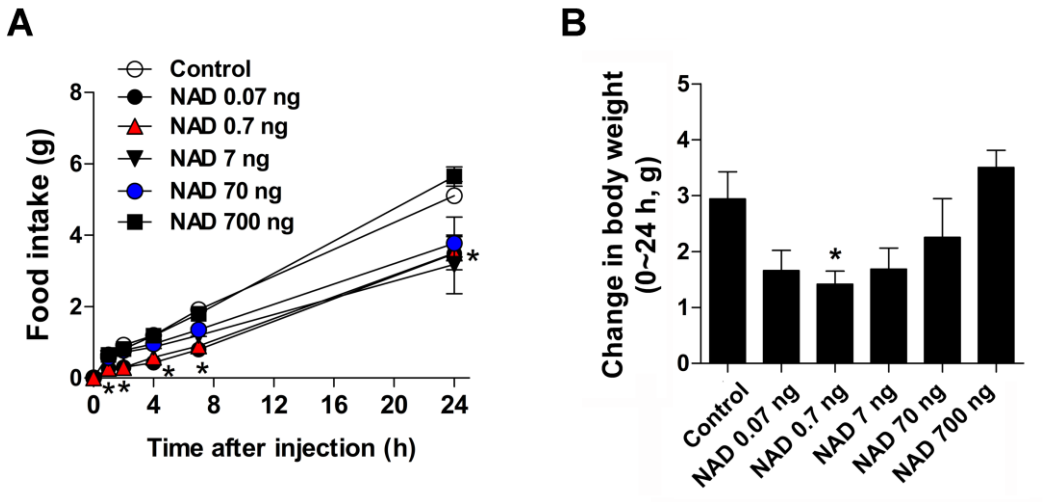

Figure 7. Dose response study of NAD. (A) Food intake and (B) body weight changes for 24 h after ICV injection of NAD at the indicated doses (n = 6). Saline or NAD was administered into the cerebroventricle of overnight-fasted mice. Results are presented as mean ± SEM. **P* < 0.05 vs. control.

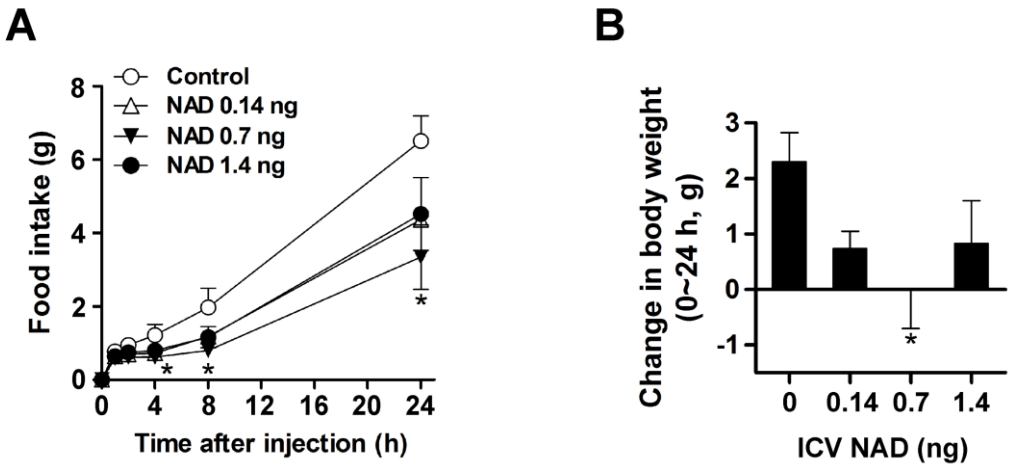

Figure 8. The anorexigenic effect of centrally administered NAD. (A) Food intake and (B) changes in body weight for 24 h after ICV injection of NAD at the indicated doses (n = 6). Mice were fasted overnight before the injections. Results are presented as mean ± SEM. *P < 0.05 vs. control.

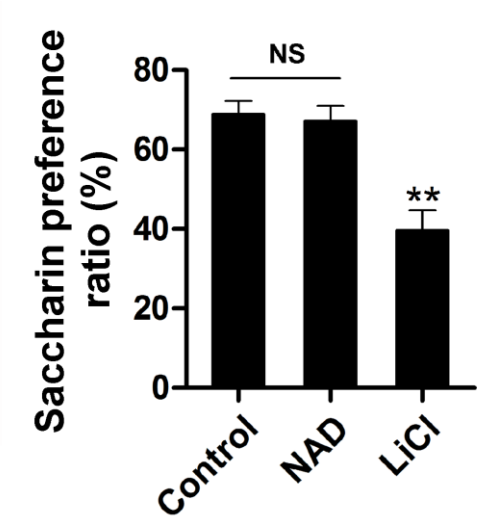

Figure 9. Conditioned taste aversion test. Effect of ICV injection of NAD (0.7 ng) or IP injection of lithium chloride (200 mg/kg) on saccharin preference ratio (n = 8). Lithium chloride, a well-known CTA inducer, induced conditioned taste aversion. Results are presented as mean ± SEM. $^{**}P < 0.01$ vs. control. NS: not significant.

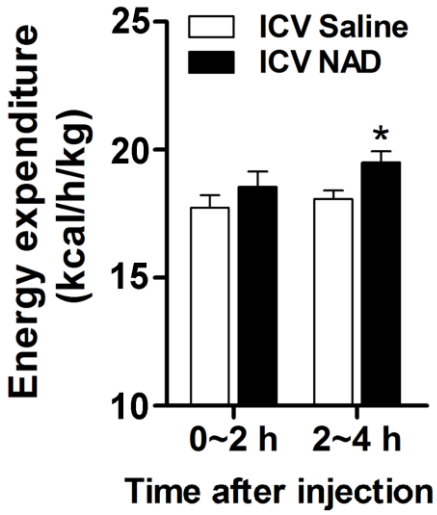

Figure 10. Effects of ICV administration of NAD on energy expenditure for indicated periods. Energy expenditure was measured using a comprehensive lab monitoring system (CLAMS). Either saline or NAD (0.7 ng) was administered ICV in the early light phase, and EE was monitored for four hours following NAD injection (n = 6). Results are presented as mean ± SEM. **P* < 0.05 vs. control.

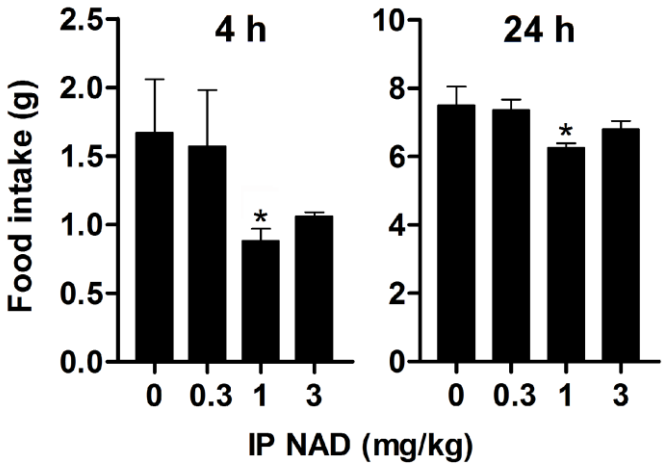

Figure 11. The anorexigenic effect of peripherally administered NAD. Food intakes were measured for the 4 and 24 h period after IP NAD administration (0.3, 1, 3 mg/kg) in overnight fasted mice (n = 6). Results are presented as mean ± SEM. **P* < 0.05 vs. control.

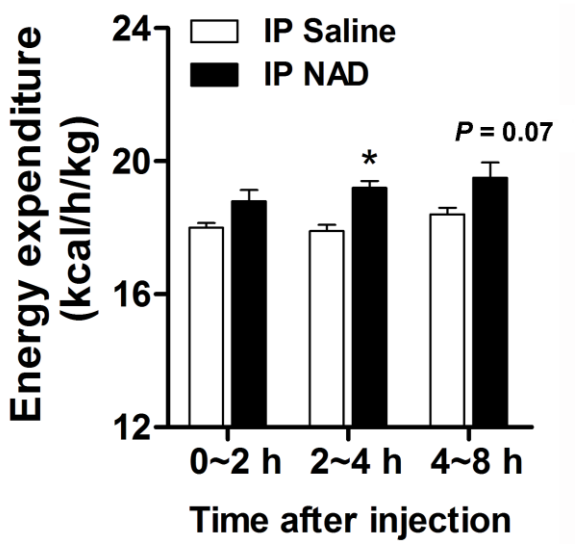

Figure 12. Effects of IP administration of NAD on energy expenditure. Either saline or NAD (1 mg/kg) was administered IP in the early light phase, and EE was monitored for eight hours following NAD injection (n = 6). Results are presented as mean ± SEM. **P* < 0.05 vs. control.

3.3. Hypothalamic Cx43 is critical for the metabolic effects of exogenous NAD

I studied if the hypothalamic gap junction protein Cx43 mediates the metabolic effects of NAD. Consistent with our previous observation on *in vitro* NAD uptake, prior ICV injection of gap junction inhibitor CBN blocked NAD-induced anorexia, whereas CD73 inhibitor CMP injection did not (Figure 13). ICV NAD administration in mice significantly increased NAD contents in the MBH 1 h after injection, which was inhibited by prior ICV injection of CBN but not by CMP (Figure 14). I tested the effects of hypothalamic Cx43 knockdown in vivo by injecting Cx43 siRNA into the bilateral ARC of mice. MBH injection with Cx43 siRNA decreased Cx43 mRNA expression by more than 50% to the average level of control siRNA-injected controls (Figure 15). In mice with reduced hypothalamic Cx43 expression, the effects of ICV- and IP-administered NAD on food intake and MBH NAD levels were significantly blunted (Figure 16 and Figure 17). Consistently, prior ICV injection of CBN or ARC injection of Cx43 siRNA significantly diminished the hypothalamic uptake

of FITC-NAD (Figure 18A and B). All these findings indicate that exogenous NAD is effectively transported into the hypothalamic neurons via Cx43.

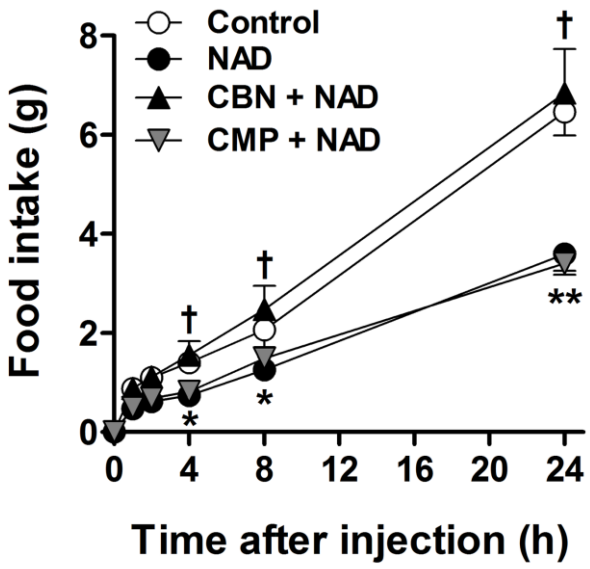

Figure 13. Hypothalamic inhibition of gap junction blocks the anorexigenic effect of exogenous NAD. Effects of ICV injection of gap junction inhibitor CBN (0.1 μg) or CD73 inhibitor CMP (0.2 μg) on NAD (0.7 ng)-induced anorexia (n = 5–6). Results are presented as mean ± SEM. **P* < 0.05, ***P* < 0.01 vs. control. †*P* < 0.05 vs. NAD alone.

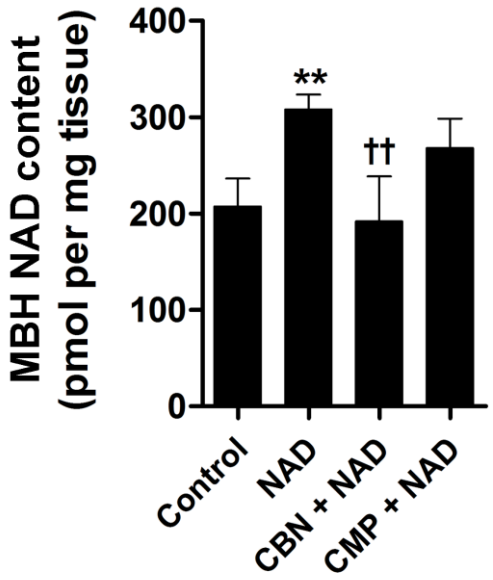

Figure 14. Hypothalamic inhibition of gap junction blocks the increased MBH NAD contents induced by exogenous NAD. Effects of ICV injection of gap junction inhibitor CBN (0.1 μg) or CD73 inhibitor CMP (0.2 μg) on NAD (0.7 ng)-induced increased MBH NAD content (n = 5–6). Results are presented as mean ± SEM. $^{**}P < 0.01$ vs. control. $^{\dagger\dagger}P < 0.01$ vs. NAD alone.

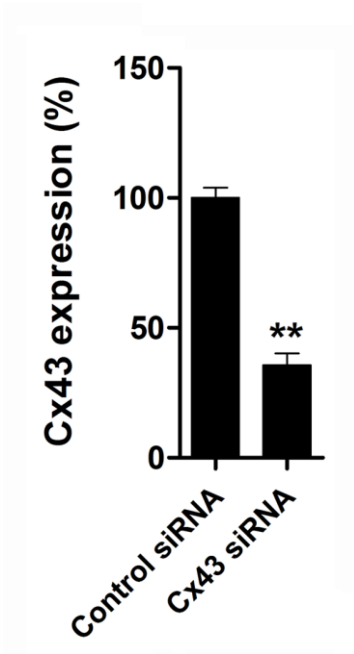

Figure 15. Knockdown of Cx43 mRNA expression by microinjecting Cx43 siRNA into the bilateral MBH. MBH Cx43 mRNA expression after intra-ARC injection of Cx43 siRNA (n = 10–12). Knockdown was considered successful if MBH Cx43 mRNA or protein expression decreased by >50% of the average Cx43 expression in controls. Only the animals with successful knockdown were included in data analysis.

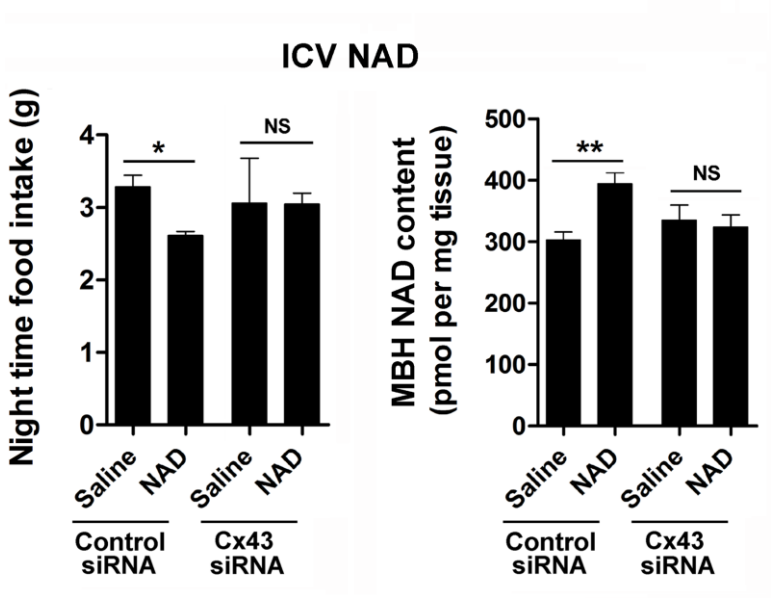

Figure 16. Hypothalamic inhibition of Cx43 blocks the metabolic effects of ICV injected NAD. Effect of ICV NAD (0.7 ng) on nighttime food intake and MBH NAD contents in mice with bilateral intra-ARC injection of control siRNA or Cx43 siRNA (n = 4–5). Under anesthesia, Cx43 siRNA (0.5 nmol in 500 nl/each injection site) was microinjected bilaterally into the ARC. Nighttime food intake was measured on the second day after siRNA injection following ICV injection of saline or NAD (0.7 μg) 1 h before light-off. In the morning of the 3rd post-injection day, mice were sacrificed to collect hypothalamic block or whole brain 1 h after ICV injection of NAD (0.7 ng). Results are presented as mean ± SEM. **P* < 0.05, ***P* < 0.01 vs. control. NS: not significant.

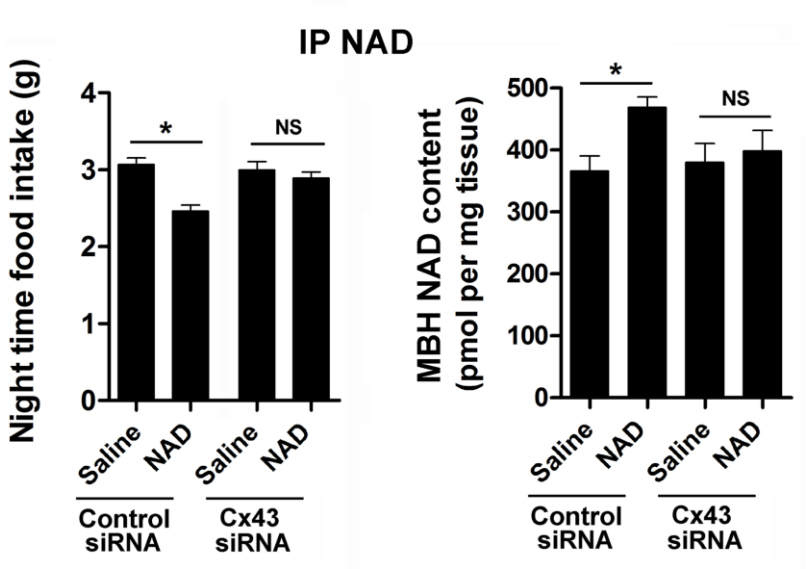

Figure 17. Hypothalamic inhibition of Cx43 blocks the metabolic effects of IP injected NAD. Effect of IP NAD (1 mg/kg) on nighttime food intake and MBH NAD contents in mice with bilateral intra-ARC injection of control siRNA or Cx43 siRNA (n = 4–5). On the second day after Cx43 siRNA injection (0.5 nmol in 500 nl/each injection site), nighttime food intake was measured following IP injection of saline or NAD (1 mg/kg) 1 h before light-off. In the morning of the 3rd post-injection day, mice were sacrificed to collect hypothalamic block or whole brain 1 h after IP injection of NAD (1 mg/kg). Results are presented as mean ± SEM. **P* < 0.05, ***P* < 0.01 vs. control. NS: not significant.

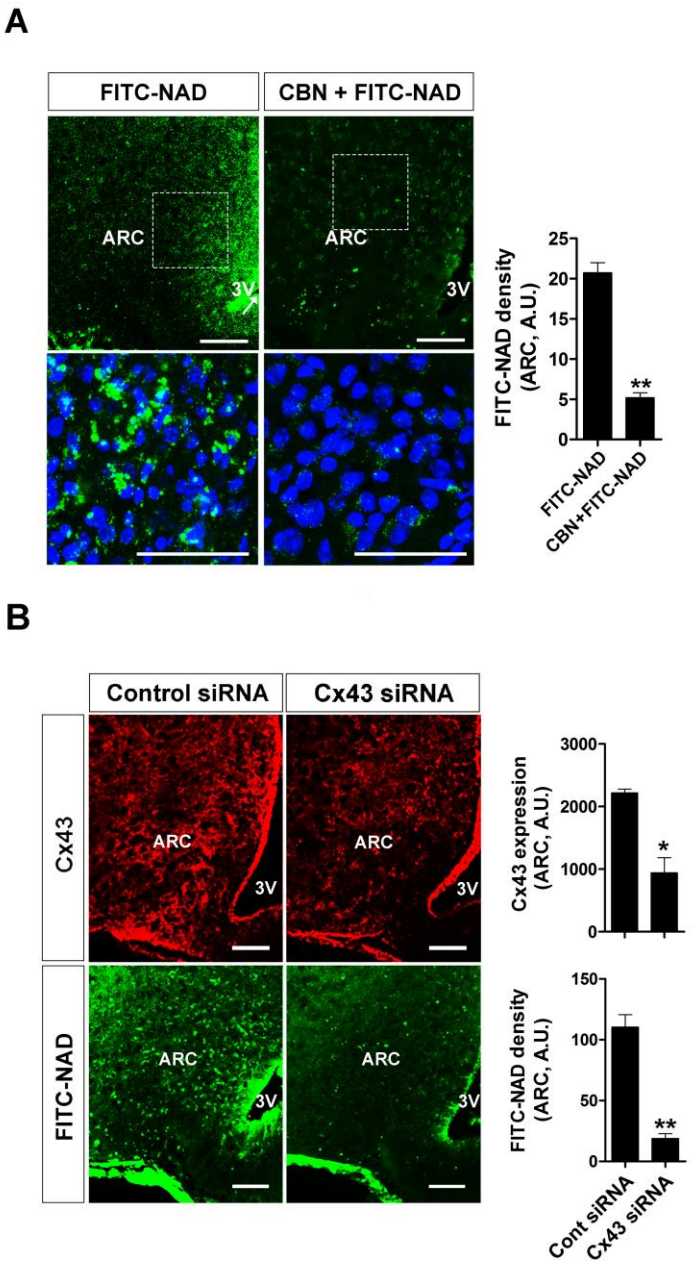

Figure 18. Hypothalamic inhibition of gap junction and Cx43 blocks hypothalamic uptake of FITC-NAD. (A) FITC-NAD signals in the ARC of mice with ICV injection of FITC-NAD alone or together with CBN (0.1 μg). (B) Cx43 immunohistochemistry and FITC-NAD signals in the ARC of mice injected with control siRNA or Cx43 siRNA in bilateral ARC (n = 4–5). FITC-labeled NAD (250 pmol in 2 μl) was administered via ICV-implanted cannulae. One hour after injection, whole brain was obtained to examine hypothalamic uptake of FITC-NAD. Scale bar: 50 μm. Results are presented as mean ± SEM. **P* < 0.05, ***P* < 0.01 vs. control.

3.4. Extracellular NAD regulates NPY and AgRP transcription in a SIRT1-dependent manner

I explored the mechanisms by which NAD regulates food intake and body weight. ICV administration of NAD in overnight-fasted mice decreased the mRNA expression of orexigenic NPY and AgRP mRNA in the ARC (Figure 19). Conversely, POMC, SIRT1 and SIRT3 mRNA expression in the ARC were not significantly altered by ICV NAD injection (Figure 19).

I further investigated the effect of extracellular NAD treatment on the transcriptional activities of AgRP, NPY, and POMC *in vitro*. NPY and AgRP promoter activity was significantly decreased by NAD (0.1 and 10 nM) treatment (Figure 20). Consistently, NPY and AgRP promoter activity was increased by FK866 (10 nM) treatment, which inhibits the rate limiting step of NAD salvage pathway and induces intracellular NAD depletion. In contrast, POMC promoter activity was not altered by NAD treatment, but reduced by FK866 (Figure 20). These findings suggest that exogenous NAD may modulate energy metabolism,

at least in part, through transcriptional suppression of NPY and AgRP.

Considering the important role of hypothalamic sirtuins, especially SIRT1, in central regulation of energy metabolism [39], I tested the role of hypothalamic sirtuins mediating the NAD actions. Co-treatment of the general sirtuin inhibitor sirtinol and SIRT1-specific inhibitor EX527 blocked the NAD-induced decrease on NPY promoter activity (Figure 21), indicating that transcriptional regulation of NPY by NAD occurs through SIRT1-dependent mechanisms. FOXO1 is an important transcriptional regulator of NPY [33] and FOXO1's transcriptional activity is modulated by SIRT-mediated deacetylation in the peripheral metabolic organs [40]. Notably, NAD treatment was unable to suppress NPY promoter activity when FOXO1 binding sites IRE2 and IRE3 in the NPY promoter region were deleted (Figure 22). These data imply that NAD regulates NPY transcription through FOXO1. Consistently, prior ICV administration of sirtinol or EX527 significantly blocked NAD-induced reduction in food intake and body weight (Figure 23A and B).

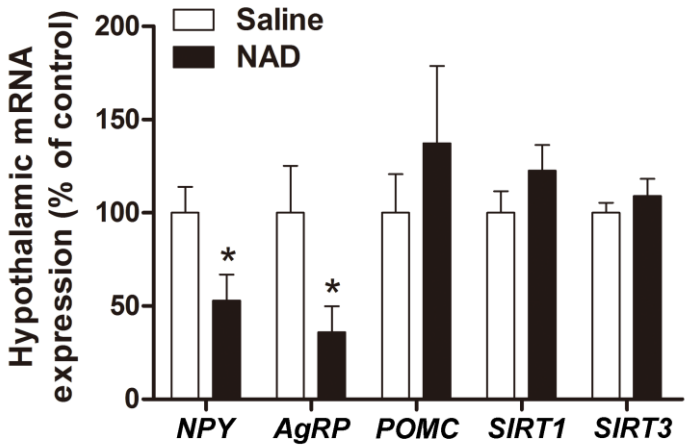

Figure 19. Effect of ICV injection of NAD on the mRNA expression levels of appetite regulating neuropeptides and sirtuins in the hypothalamic ARC. Mouse hypothalamic ARC was collected after 1 h of ICV injection of NAD (0.7 ng) using the micropunch technique using a Harvard brain matrix and blunted 20 gauge-metal needles (inner dimeter 0.91 mm) (n = 8). Bilateral ARC was collected from two consecutive brain slices. The thickness of brain slice was 1 mm. mRNA expression was determined by real-time PCR analysis. Results are presented as mean ± SEM. **P* < 0.05 vs. control.

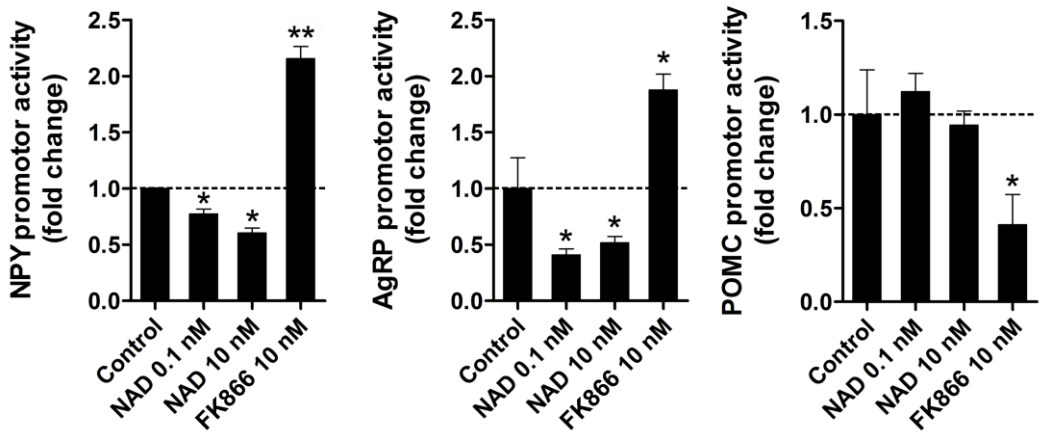

Figure 20. Effects of NAD and FK866 treatment on the transcriptional activities of NPY, AgRP, and POMC. To investigate the effect of extracellular NAD treatment on the transcriptional activities of AgRP, NPY, and POMC *in vitro*, promoter assay of human AgRP, NPY, and POMC was performed. SHSY-5Y cells for NPY and AgRP promoter analysis and AtT20 cells for POMC promoter analysis were transfected with pNPY-luc, pAgRP-luc or pPOMC-luc (50 ng) using Lipofectamine. Forty-eight hours after transfection, cells were treated with NAD (0.1 and 10 nM) or FK866 (10 nM) for 2 h. Cells were lysed and extracted to measure luciferase activity by a luminometer and normalized for β-galactosidase activity. Results are presented as mean ± SEM. **P* < 0.05, ***P* < 0.01 vs. control.

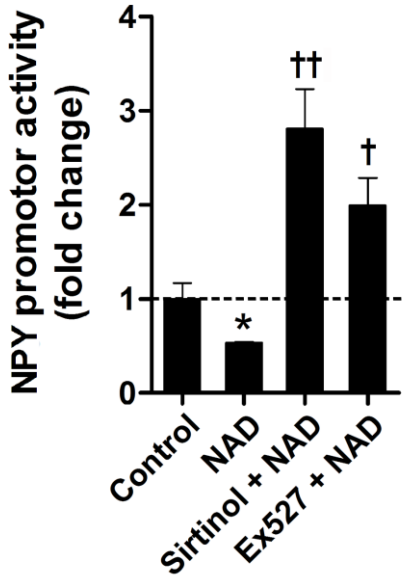

Figure 21. Effect of treatment of NAD alone or with sirtinol or EX527 on NPY promoter activity. To test the role of hypothalamic sirtuins mediating the NAD actions, promoter assay of human NPY was performed. Forty-eight hours after transfection of pNPY-luc (50 ng), cell were treated with NAD (10 nM) alone or with sirtinol (200 nM) or EX527 (100 nM) for 2 h before lysis of cells. Results are presented as mean ± SEM. **P* < 0.05 vs. control. . $^{\dagger}P < 0.05$, $^{\dagger\dagger}P < 0.01$ vs. NAD alone.

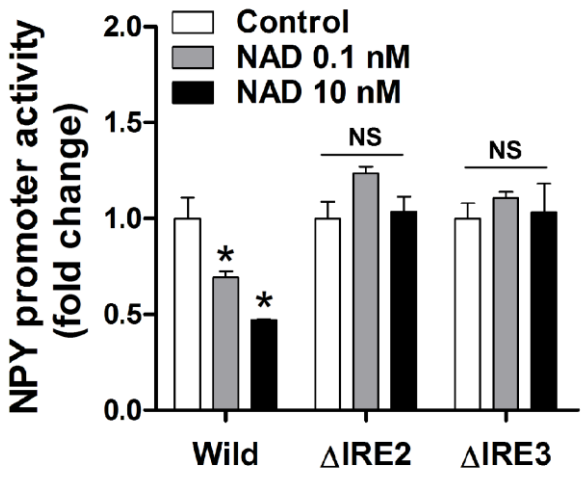

Figure 22. Effects of treatment of NAD on wild type NPY promoter or NPY promoter with deletion of FOXO1 binding sites IRE2 (ΔIRE2) and IRE3 (ΔIRE3). Since FOXO1 is an important transcriptional regulator of NPY and FOXO1's transcriptional activity is modulated by SIRT-mediated deacetylation in the peripheral metabolic organs, NPY promoter assay was performed using NPY promoter with deletion of FOXO1 binding sites. Forty-eight hours after transfection of NPY promoter, cells were treated with NAD (0.1 nM or 10 nM). Results are presented as mean ± SEM. **P* < 0.05 vs. control. NS: not significant.

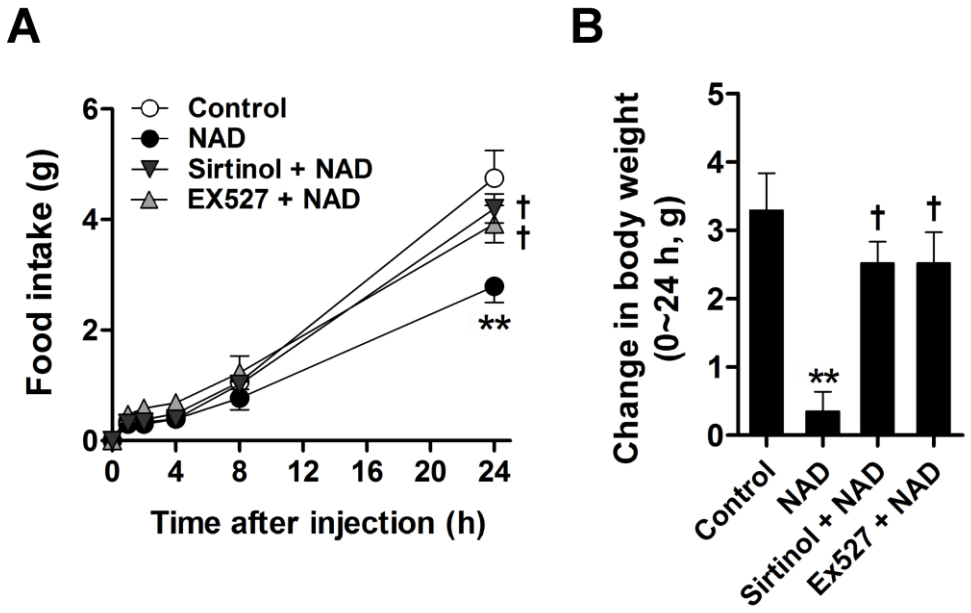

Figure 23. Hypothalamic inhibition of SIRT1 blocks the metabolic effects of exogenous NAD. (A) Food intakes and (B) body weight changes for the 24 h period following ICV administration of NAD (0.7 ng) alone or together with sirtinol (200 ng) or EX527 (100 ng) (n = 6). Results are presented as mean ± SEM. **P* < 0.05 vs. control.

3.5. Chronic NAD supplementation rescues blunted circadian rhythms in DIO mice

I finally investigated the beneficial metabolic effects of chronic NAD supplementation in both lean mice and HFD-fed DIO mice. Mice were daily injected with either saline or NAD (1 mg/kg) intraperitoneally for 4 weeks before light-off. In contrast to acute NAD treatment, chronic NAD treatment had no effect on body weights in lean mice (Figure 24). However, it significantly prevented weight gain in HFD-fed mice (Figure 24). I measured EE and locomotor activity immediately after the completion of NAD treatment, and observed that compared to normal lean mice, DIO mice showed decreased EE and reduced locomotor activity, especially during nighttime (Figure 25A and B). Chronic NAD supplement partially rescued nighttime reduction in EE and locomotor activity in DIO mice (Figure 25 A and B). Both daytime and nighttime food intakes were greater in DIO mice than in lean controls. Moreover, DIO mice showed increased proportion of daytime calorie intake (32.9 ± 1.2 % vs. lean 12.2 ± 3.99 %, $P < 0.01$) (Figure 26), suggesting blunted

circadian rhythms in food intake in obese mice. NAD supplement in obese mice significantly reduced daytime food intake and partially corrected the increased daytime calorie intake (Figure 26). MBH NAD contents at the end of study period were lower in NAD-untreated DIO mice, which were almost normalized by exogenous NAD supply (Figure 27).

Given the significant impact of exogenous NAD on circadian rhythms of metabolic behaviors, I tested the effect of exogenous NAD on the promoter activity of clock gene PER1. NAD depletion induced by FK866 treatment decreased BMAL1/CLOCK-stimulated PER1 transcription (Figure 28). Co-treatment of NAD prevented FK866-induced suppression in PER1 transcriptional activity, although these treatments had no significant effect on basal PER1 promoter activity (Figure 28). These results imply that exogenous NAD can reverse the suppression of transcriptional activity of key clock genes by cellular NAD depletion. Given the NAD regulation of both NPY/AgRP and PER1 transcription, I finally tested any possible interaction between clock genes and NPY/AgRP transcription. NPY and AgRP promoter activities were significantly suppressed by overexpression of

BMAL1/CLOCK (Figure 29) and stimulated by overexpression of PER1 and PER2 (Figure 30). Taken together, exogenous NAD-mediated clock gene regulation may help diurnal fluctuations in hypothalamic NPY/AgRP expression and thus diurnal rhythms of metabolic behaviors.

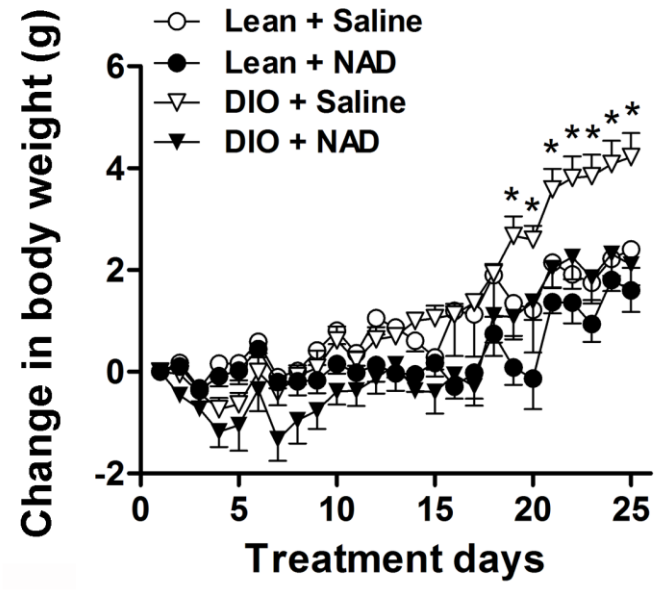

Figure 24. Effects of chronic NAD supplementation on body weight gain in DIO mice. For chronic NAD treatment, NAD (1 mg/kg) was daily injected intraperitoneally at 1 h before light-off for 4 weeks (n = 6–7 for each group). Body weight was daily monitored before NAD injection .*$P < 0.05$ vs. saline-treated lean mice.

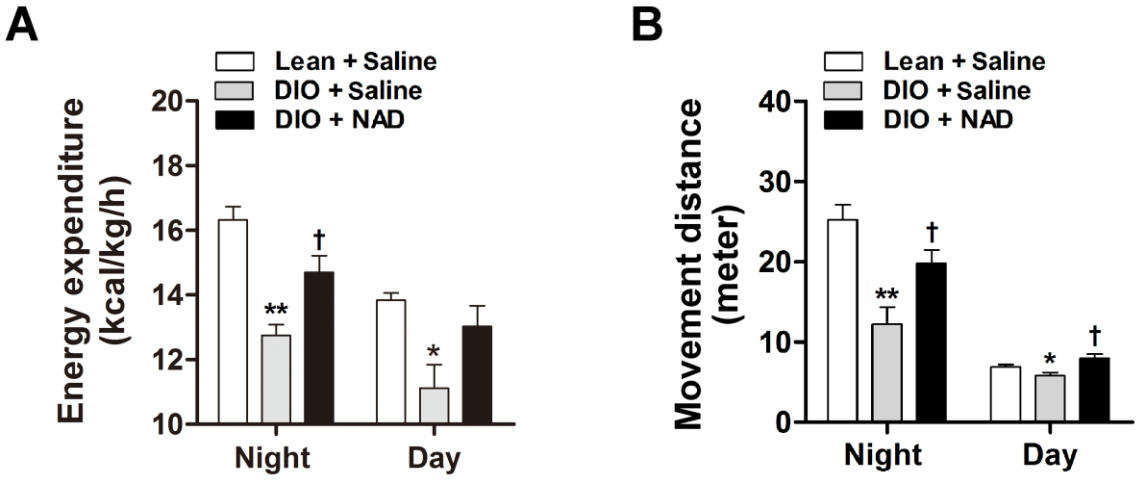

Figure 25. Effects of chronic NAD supplementation on energy expenditure and locomotor acdtivity in DIO mice. Circadian patterns of energy expenditure and locomotor activity were monitored at the end of the study in lean mice and DIO mice with or without 4 weeks-NAD supplementation (n = 6–7). *$P < 0.05$, **$P < 0.01$ vs. control. $^{\dagger}P < 0.05$ vs. saline-treated DIO mice.

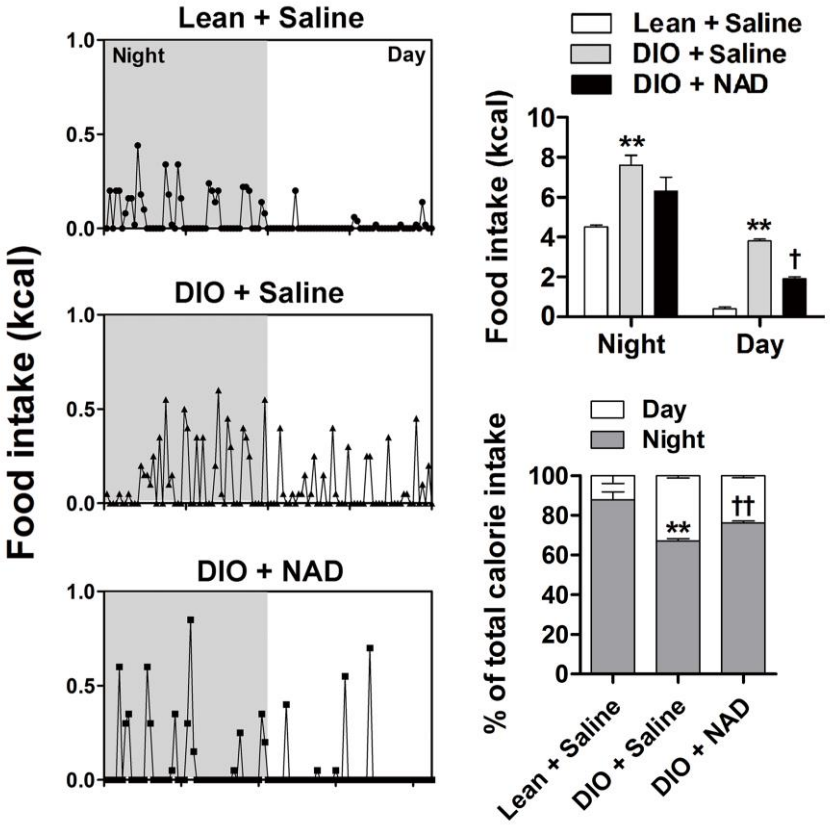

Figure 26. Effects of chronic NAD supplementation on food consumption in DIO mice. Circadian patterns of food intake and feeding frequency were monitored at the end of the study in lean mice and DIO mice with or without 4 weeks-NAD supplementation (n = 6–7). **P* < 0.05, ***P* < 0.01 vs. control. †*P* < 0.05 vs. saline-treated DIO mice.

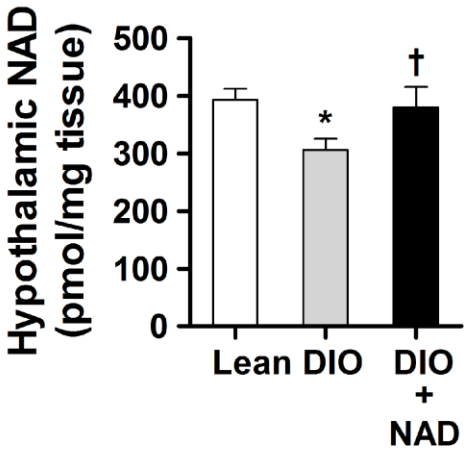

Figure 27. MBH NAD contents in in lean mice and DIO mice with or without 4 weeks-NAD supplementation. MBH NAD contents were measured using HPLC at the end of study period in lean mice and DIO mice with or without 4 weeks-NAD supplementation (n = 6–7). **P* < 0.05 vs. control. †*P* < 0.05 vs. saline-treated DIO mice.

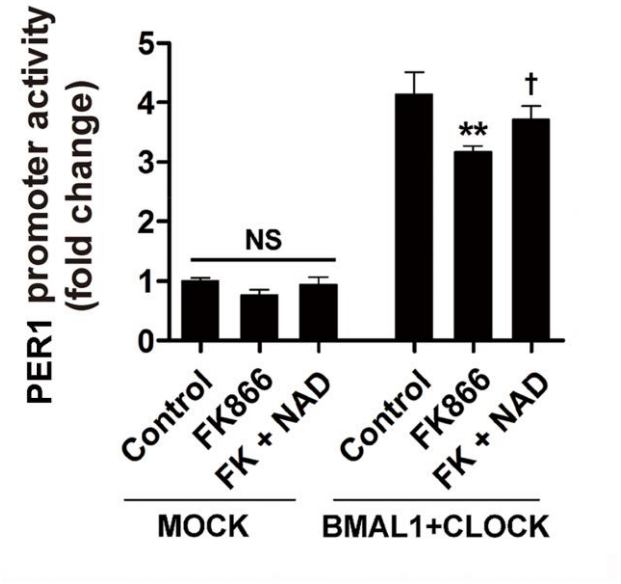

Figure 28. Basal and BMAL1/CLOCK-stimulated PER1 promoter activity in N1 cells treated with FK866 alone or with NAD. The effect of exogenous NAD on the promoter activity of clock gene PER1 was tested. For period 1 (PER1) promoter analysis, N1 cells were transfected with mPER1 promoter-luciferase construct and/or plasmids expressing mBMAL1 and mCLOCK, and β-galactosidase (50 ng). Forty-eight hours after transfection, cells were treated with FK866 (10 nM) with or without NAD (10 nM) for 2 h. $^{**}P < 0.01$ vs. control. $^{\dagger}P < 0.05$ vs. FK866 alone group. NS: not significant.

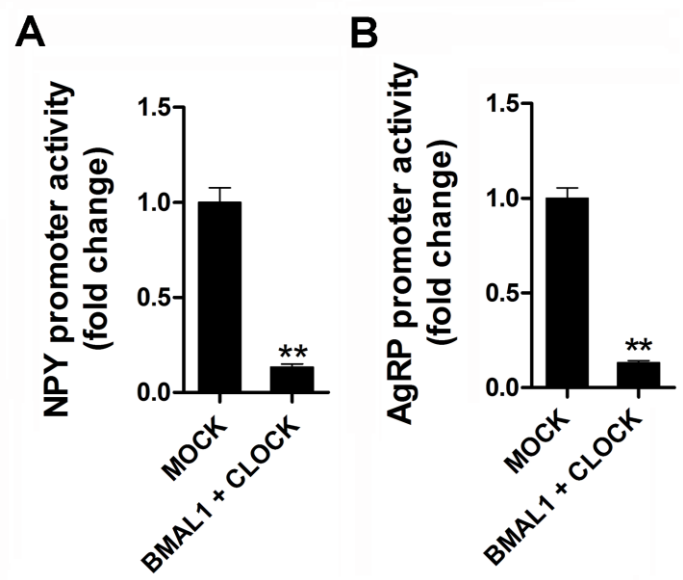

Figure 29. Effects of BMA1/CLOCK overexpression on NPY and AgRP transcriptional activities. To study the effect of clock genes on the NPY and AgRP promotor activity, cells were transfected with NPY or AgRP promoter-luciferase construct and/or plasmids expressing mBMAL1 and mCLOCK, and β-galactosidase (50 ng). Forty-eight hours after transfection, cells were lysed and extracted to measure luciferase activity. $^{**}P < 0.01$ vs. control.

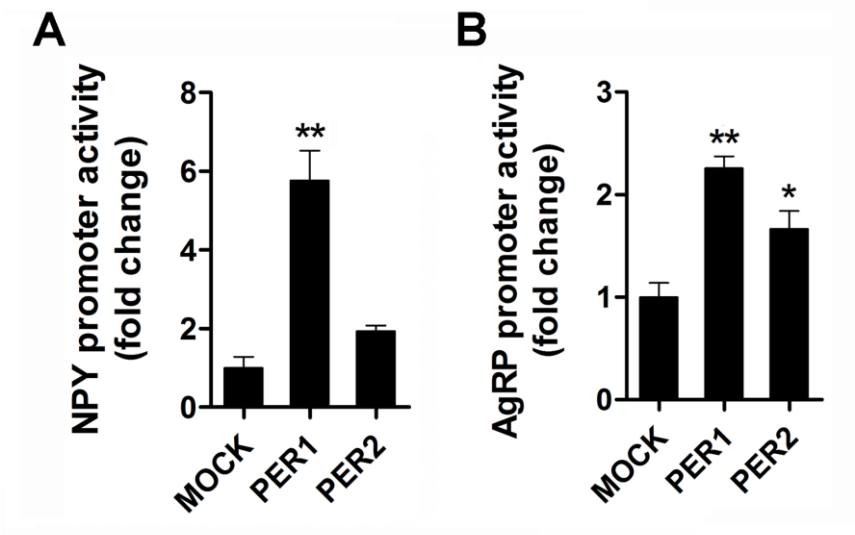

Figure 30. Effects of PER1 or PER2 overexpression on NPY and AgRP transcriptional activities. To study the effect of clock genes on the NPY and AgRP promotor activity, cells were transfected with NPY or AgRP promoter-luciferase construct and/or plasmids expressing mPER1 or mPER2 and β-galactosidase (50 ng). Forty-eight hours after transfection, cells were lysed and extracted to measure luciferase activity. $^{**}P < 0.01$ vs. control.

4. Discussion

In this study, I demonstrated using mice that supplementation with NAD effectively increased hypothalamic NAD content and has a therapeutic benefit in controlling energy metabolism. Acute central and peripheral administration of NAD suppressed fasting-induced hyperphagia and weight gain in normal mice. Chronic administration of NAD significantly attenuated weight gain in HFD-fed DIO mice without any observable adverse effects.

Previous studies reported the beneficial metabolic effects of the supplement with NAD precursor NR and NMN in obese and aged mice and humans [28, 32, 41-43]. Administration of NMN (500 mg/kg/day IP) for one week improved glucose metabolism in diabetic mice [32] and restored mitochondrial homeostasis in muscles of aged mice [28]. Twelve month-long NMN administration to mice (100 to 300 mg/kg in drinking water) attenuated aging-associated body weight gain [42]. On the other hand, 12 week-supplementation with NR (400 mg/kg/day in drinking water) reduced body weight gain and fat mass and increased energy expenditure in HFD-fed mice [41]. Of note, the effective dose of IP-administered

NAD (1 mg/kg) was more than 100 times lower than the effective dose of IP NMN [28, 31, 32]. Moreover, NAD dose-response studies showed a bell-shaped response curve with the greatest effect seen in very low dose of NAD (1 mg/kg for IP administration and 0.7 ng per animal for ICV administration). The mechanism underlying this observation is yet to be clarified. I assume that supplementation with higher NAD doses could increase intracellular or extracellular NAD levels to the supraphysiologic levels and activate the pathways which degrade NAD to offset the beneficial effects of NAD. As such, chronic NAD supply in lean mice with adequate cellular NAD levels had no significant effect on body weight.

It has been suggested the possibility that exogenous NMN or NAD is extracellularly converted to NR by ecto-5'-nucleotidase CD73 and then enters cells via nucleoside transporters [29]. Therefore, I tested if CD73 is required for hypothalamic NAD uptake and biological actions of NAD. Blockade of CD73 using CMP and APCP failed to block the effects of exogenous NAD. Moreover, I directly showed cellular uptake of FITC-NAD; because FITC was bound to the adenine residue of NAD, NMN produced from exogenous NAD was not labeled with FITC and not detected as FITC signal. These findings suggest a

direct transport of exogenous NAD to hypothalamic neurons.

Connexin inhibitors were shown to block the uptake of isotope-labeled NAD in mammalian cells [44]. Consistently, I found that connexin inhibitor CBN completely blocked the effects of exogenous NAD on hypothalamic NAD levels, food intake, and body weight. More importantly, I found high expression of Cx43 in the mouse hypothalamus, and inhibition of hypothalamic Cx43 expression effectively blocked hypothalamic uptake of NAD as well as the anorexigenic effects of NAD. Collectively, these data strongly indicate an important role of gap junction, especially Cx43, in NAD trafficking through the plasma membrane of hypothalamus neurons. Interestingly, a recent paper has shown an important role of Cx43 in white adipose tissue browning by mediating cell-to-cell cAMP transfer upon sympathetic activation [45]. Thus, it will be worthwhile to study other physiological functions of hypothalamic neuronal Cx43.

In this study, acute ICV injection of NAD significantly decreased hypothalamic NPY/AgRP mRNA expression. Moreover, NAD treatment suppressed the promoter activity of NPY- or AgRP-encoding genes *in vitro*, suggesting that exogenous NAD may influence

energy balance through an effect on transcription of key orexigenic neuropeptides NPY and AgRP. SIRT1 is an NAD-dependent protein deacetylase that serves as a cellular energy sensor [5]. Previous studies demonstrated that lack of SIRT1 in hypothalamic neurons leads to impaired function of hypothalamic neurons, indicating a critical role for SIRT1 in normal physiology. In our study, prior ICV administration of sirtuin inhibitor sirtinol and SIRT1 inhibitor EX527 significantly inhibited the effects of exogenous NAD on food intake and body weight, suggesting that NAD actions were mediated through hypothalamic sirtuins. SIRT1 or SIRT2 deacetylates and modulates transcriptional factor FOXO1 in the liver and adipocytes [46, 47]. FOXO1 is an important regulator of NPY transcription via direct binding to IRE sites in the promoter region [33]. Thus, I tested the involvement of FOXO1 in the NAD regulation of NPY transcription. Interestingly, NAD treatment did not suppress NPY promoter activity when FOXO1 binding sites (IREs) in the NPY promoter region were deleted. Therefore, FOXO1 binding to the NPY promoter region may be critical for the inhibition of NPY transcription by exogenous NAD.

Previous studies demonstrated that the NAMPT-NAD-SIRT1 axis regulates cellular

clockwork [12, 19, 48]. In our study, cellular NAD depletion inhibited BMAL1/CLOCK-promoted PER1 transcription in hypothalamic neuronal cells, which was reversed by exogenous supply of NAD. I also found that overexpression of CLOCK/BMAL1 potently suppressed NPY/AgRP transcriptional activity, while PER1/PER2 stimulated the same. These results may suggest that exogenous NAD indirectly controls NPY/AgRP transcription through clock gene regulation. These findings further suggest the possibility that exogenous NAD may help recover blunted diurnal fluctuations in metabolic behaviors in obese mice through interactive regulation of clock genes and NPY/AgRP. In support of this notion, NAD supplement significantly corrected blunted circadian rhythms and partially reversed the reduced nighttime physical activity and the increased daytime eating. Disrupted circadian rhythms are also found in human obesity and have adverse impacts on human health [49]. As reduced hypothalamic NAD levels in DIO mice was rescued by chronic NAD treatment, NAD supplementation has a therapeutic potential in obese patients with altered circadian behaviors.

5. Conclusions

Adequate amount of hypothalamic NAD has been reported to be critical for maintaining energy homeostasis and circadian rhythms by affecting the activity of NAD-dependent deacetylase SIRT1. Therapeutic strategies activating the cellular NAD-SIRT1 axis have been actively investigated. Previous studies have shown that supplementation with NAD precursors nicotinamide mononucleotide (NMN) and nicotinamide ribose (NR) have beneficial metabolic effects in obese or aged mice by restoring NAD levels in peripheral metabolic organs.

In this study, I showed that extracellular NAD was effectively transferred into the hypothalamic neurons via gap junction protein connexin 43. I also observed that exogenous NAD significantly modulated the transcriptional activity of hypothalamic NPY, AgRP, and Period 1 genes. Transcriptional regulation of NPY by NAD occurred through SIRT1-FOXO1-dependent mechanisms. I further demonstrated that central and peripheral administration of NAD suppressed fasting-induced hyperphagia and weight gain. Moreover,

NAD supplementation for 1 month in obese mice significantly reversed blunted circadian rhythm of feeding behavior, locomotor activity, and energy expenditure, along with correction of hypothalamic NAD deficit.

This is the first study to demonstrate the therapeutic potential of low-dose NAD supplementation in obese mice with altered circadian behaviors. I also show for the first time that exogenous NAD is transported into hypothalamic neurons in vivo via gap junction protein connexin 43, where it regulates the transcriptional activities of NPY, AgRP, and PER1 genes.

6. References

1. Belenky, P., K.L. Bogan, and C. Brenner, *NAD+ metabolism in health and disease.* Trends in biochemical sciences, 2007. **32**(1): p. 12-19.

2. Lin, S.-J. and L. Guarente, *Nicotinamide adenine dinucleotide, a metabolic regulator of transcription, longevity and disease.* Current opinion in cell biology, 2003. **15**(2): p. 241-246.

3. Imai, S.-i. and L. Guarente, *NAD+ and sirtuins in aging and disease.* Trends in cell biology, 2014. **24**(8): p. 464-471.

4. Canto, C., K.J. Menzies, and J. Auwerx, *NAD+ metabolism and the control of energy homeostasis: A balancing act between mitochondria and the nucleus.* Cell metabolism, 2015. **22**(1): p. 31-53.

5. Haigis, M.C. and D.A. Sinclair, *Mammalian sirtuins: biological insights and disease relevance*. Annual review of pathology, 2010. **5**: p. 253-295.

6. Tissenbaum, H.A. and L. Guarente, *Increased dosage of a sir-2 gene extends lifespan in Caenorhabditis elegans.* Nature, 2001. **410**(6825): p. 227-230.

7. Picard, F., et al., *Sirt1 promotes fat mobilization in white adipocytes by repressing PPAR-γ.* Nature, 2004. **429**(6993): p. 771-776.

8. Brunet, A., et al., *Stress-dependent regulation of FOXO transcription factors by the SIRT1 deacetylase*. Science, 2004. **303**(5666): p. 2011-2015.

9. Rodgers, J.T., et al., *Nutrient control of glucose homeostasis through a complex of PGC-1α and SIRT1.* Nature, 2005. **434**(7029): p. 113-118.

10. Preiss, J. and P. Handler, *Biosynthesis of diphosphopyridine nucleotide.* J. biol. Chem, 1958. **233**: p. 493-500.

11. Çakir, I., et al., *Hypothalamic Sirt1 regulates food intake in a rodent model system.* PloS one, 2009. **4**(12): p. e8322.

12. Nakahata, Y., et al., *Circadian control of the NAD+ salvage pathway by CLOCK-SIRT1.* Science, 2009. **324**(5927): p. 654-657.

13. Ramadori, G., et al., *SIRT1 deacetylase in POMC neurons is required for homeostatic defenses against diet-induced obesity.* Cell metabolism, 2010. **12**(1): p. 78-87.

14. Dietrich, M.O., et al., *Agrp neurons mediate Sirt1's action on the melanocortin system and energy balance: roles for Sirt1 in neuronal firing and synaptic plasticity.* The Journal of Neuroscience, 2010. **30**(35): p. 11815-11825.

15. Coppari, R., *Metabolic actions of hypothalamic SIRT1.* Trends in Endocrinology & Metabolism, 2012. **23**(4): p. 179-185.

16. Ramadori, G., et al., *SIRT1 deacetylase in SF1 neurons protects against metabolic imbalance.* Cell metabolism, 2011. **14**(3): p. 301-312.

17. Chang, H.-C. and L. Guarente, *SIRT1 mediates central circadian control in the SCN by a mechanism that decays with aging.* Cell, 2013. **153**(7): p. 1448-1460.

18. Nakahata, Y., et al., *The NAD+-dependent deacetylase SIRT1 modulates CLOCK-*

mediated chromatin remodeling and circadian control. Cell, 2008. **134**(2): p. 329-340.

19. Asher, G., et al., *SIRT1 regulates circadian clock gene expression through PER2 deacetylation.* Cell, 2008. **134**(2): p. 317-328.

20. Sasaki, T., et al., *Hypothalamic SIRT1 prevents age-associated weight gain by improving leptin sensitivity in mice.* Diabetologia, 2014. **57**(4): p. 819-831.

21. Chang, H.-C. and L. Guarente, *SIRT1 and other sirtuins in metabolism.* Trends in Endocrinology & Metabolism, 2014. **25**(3): p. 138-145.

22. Lagouge, M., et al., *Resveratrol improves mitochondrial function and protects against metabolic disease by activating SIRT1 and PGC-1α.* Cell, 2006. **127**(6): p. 1109-1122.

23. Baur, J.A., et al., *Resveratrol improves health and survival of mice on a high-calorie diet.* Nature, 2006. **444**(7117): p. 337-342.

24. Minor, R.K., et al., *SRT1720 improves survival and healthspan of obese mice.* Scientific reports, 2011. **1**.

25. Sinclair, D.A. and L. Guarente, *Small-molecule allosteric activators of sirtuins.* Annual review of pharmacology and toxicology, 2014. **54**: p. 363-380.

26. Belenky, P., et al., *Nicotinamide riboside promotes Sir2 silencing and extends lifespan via Nrk and Urh1/Pnp1/Meu1 pathways to NAD+*. Cell, 2007. **129**(3): p. 473-484.

27. Bogan, K.L. and C. Brenner, *Nicotinic acid, nicotinamide, and nicotinamide riboside:*

a molecular evaluation of NAD+ precursor vitamins in human nutrition. Annu. Rev. Nutr., 2008. **28**: p. 115-130.

28. Gomes, A.P., et al., *Declining NAD+ induces a pseudohypoxic state disrupting nuclear-mitochondrial communication during aging.* Cell, 2013. **155**(7): p. 1624-1638.

29. Ratajczak, J., et al., *NRK1 controls nicotinamide mononucleotide and nicotinamide riboside metabolism in mammalian cells.* Nature Communications, 2016. **7**: p. 13103.

30. Zhou, M., et al., *Neuronal death induced by misfolded prion protein is due to NAD+ depletion and can be relieved in vitro and in vivo by NAD+ replenishment.* Brain, 2015. **138**(4): p. 992-1008.

31. Ramsey, K.M., et al., *Age-associated loss of Sirt1-mediated enhancement of glucose-stimulated insulin secretion in beta cell-specific Sirt1-overexpressing (BESTO) mice.* Aging cell, 2008. **7**(1): p. 78-88.

32. Yoshino, J., et al., *Nicotinamide mononucleotide, a key NAD+ intermediate, treats the pathophysiology of diet-and age-induced diabetes in mice.* Cell metabolism, 2011. **14**(4): p. 528-536.

33. Kim, M.-S., et al., *Role of hypothalamic Foxo1 in the regulation of food intake and energy homeostasis.* Nature neuroscience, 2006. **9**(7): p. 901-906.

34. Minokoshi, Y., et al., *AMP-kinase regulates food intake by responding to hormonal and nutrient signals in the hypothalamus.* Nature, 2004. **428**(6982): p. 569-574.

35. Blundon, J.A., et al., *Restoring auditory cortex plasticity in adult mice by restricting thalamic adenosine signaling.* Science, 2017. **356**(6345): p. 1352-1356.

36. Hartman, M.E., et al., *An optimized and simplified system of mouse embryonic stem cell cardiac differentiation for the assessment of differentiation modifiers.* PloS one, 2014. **9**(3): p. e93033.

37. Bruzzone, S., et al., *Connexin 43 hemi channels mediate Ca2+-regulated transmembrane NAD+ fluxes in intact cells.* Faseb j, 2001. **15**(1): p. 10-12.

38. Nikiforov, A., et al., *Pathways and subcellular compartmentation of NAD biosynthesis in human cells from entry of extracellular precursors to mitochondrial NAD generation.* Journal of Biological Chemistry, 2011. **286**(24): p. 21767-21778.

39. Satoh, A. and S.-i. Imai, *Systemic regulation of mammalian ageing and longevity by brain sirtuins.* Nature communications, 2014. **5**.

40. Daitoku, H., et al., *Silent information regulator 2 potentiates Foxo1-mediated transcription through its deacetylase activity.* Proceedings of the National Academy of Sciences of the United States of America, 2004. **101**(27): p. 10042-10047.

41. Cantó, C., et al., *The NAD+ precursor nicotinamide riboside enhances oxidative metabolism and protects against high-fat diet-induced obesity.* Cell metabolism, 2012. **15**(6): p. 838-847.

42. Mills, K.F., et al., *Long-term administration of nicotinamide mononucleotide mitigates age-associated physiological decline in mice.* Cell metabolism, 2016. **24**(6): p. 795-806.

43. Tsubota, K., *The first human clinical study for NMN has started in Japan.* NPJ Aging and Mechanisms of Disease, 2016. **2**: p. 16021.

44. Billington, R.A., et al., *Characterization of NAD uptake in mammalian cells.* Journal of Biological Chemistry, 2008. **283**(10): p. 6367-6374.

45. Zhu, Y., et al., *Connexin 43 mediates white adipose tissue beiging by facilitating the propagation of sympathetic neuronal signals.* Cell Metabolism, 2016. **24**(3): p. 420-433.

46. Frescas, D., L. Valenti, and D. Accili, *Nuclear trapping of the forkhead transcription factor FoxO1 via Sirt-dependent deacetylation promotes expression of glucogenetic genes.* Journal of Biological Chemistry, 2005. **280**(21): p. 20589-20595.

47. Jing, E., S. Gesta, and C.R. Kahn, *SIRT2 regulates adipocyte differentiation through FoxO1 acetylation/deacetylation.* Cell metabolism, 2007. **6**(2): p. 105-114.

48. Belden, W.J. and J.C. Dunlap, *SIRT1 is a circadian deacetylase for core clock components.* Cell, 2008. **134**(2): p. 212-214.

49. Froy, O., *Metabolism and circadian rhythms—implications for obesity.* Endocrine reviews, 2010. **31**(1): p. 1-24.

Korean abstract

SIRT1 은 nicotinamide adenine dinucleotide (NAD) 의존적 단백질 탈아세틸화 효소로, 에너지 항상성과 일주기 리듬 조절의 중추인 시상하부의 신경세포 기능에 중요하다. 따라서 시상하부 신경세포 내 NAD 양을 적절하게 유지하는 것은 SIRT1 활성을 유지함으로써 에너지 항상성과 일주기 리듬을 유지하는데 핵심적이다. 포유류 세포에서 NAD 는 대부분 재활용 과정을 거쳐 생산되는데, NAD 를 분해하는 효소들에 의해 nicotinamide 로 분해되면 nicotinamide phosphoribosyltransferase (Nampt)에 의해 nicotinamide mononucleotide (NMN)로 전환되고 이는 nicotinamide mononucleotide adenylyltransferase (Nmnat) 에 의해 NAD 로 전환된다. 설치류에서 NAD 의 전구체인 NMN 등을 공급함으로써, NAD 가 감소하는 비만/노화와 관련한 대사 장애를 회복한 연구들이 발표된 바 있다.

본 연구에서 먼저 시상하부 N1 신경세포주에서 외부에서 공급한 NAD 가 시상하부 신경세포 내 NAD 양을 증가시킴을 확인하였고, NAD 의 세포 내로의

유입은 gap junction 단백인 connexin 43 이 매개함을 밝혔다. 이는 gap junction 억제제를 전처치하거나 connexin 43 의 small interfering RNA (siRNA)를 transfection 할 경우 세포 밖 NAD 의 세포 내 유입이 차단되는 결과를 통해 확인하였다.

다음으로 NAD 투여가 정상 마우스에서 식이 섭취, 체중, 에너지 대사에 미치는 영향을 확인하였다. NAD 를 뇌실 내로 주입하거나 복강 내로 주입할 경우 금식에 따른 과식과 체중 증가를 억제할 수 있었고, 에너지 소비 (energy expenditure)가 유의하게 증가하였다. 시상하부 신경세포 내로의 NAD 의 이동을 connexin 43 이 매개한다는 in vitro 결과와 일치하게, 뇌실 내로 gap junction 억제제를 주입하거나 시상하부 양측 궁상핵으로 connexin 43 siRNA 를 주입하면 시상하부 내로의 NAD 유입과 NAD 에 의한 식이 섭취 및 체중 조절 효과를 억제할 수 있었다.

마우스 뇌실 내로의 NAD 주입은 시상하부의 식욕증진 신경펩타이드 (orexigenic neuropeptide)인 NPY 와 AgRP 의 mRNA 발현을 감소시켰는데, 이는 in vitro 에서 NAD 의 공급이 NPY 와 AgRP 의 프로모터 활성을 억제시키는

결과와 일치하였다. 이처럼 시상하부 신경세포 외부에서 공급한 NAD 는 세포 내의 NPY 와 AgRP 전사 활성을 조절하는데, 이러한 효과는 SIRT1 과 FOXO1 을 매개로 함을 확인하였다.

마지막으로 고지방식이 섭취를 통해 비만을 유도한 마우스에서 NAD 보충이 치료적 효과가 있는지를 확인하였다. 식이 유도 비만 마우스는 정상 마우스에 비해 시상하부 NAD 양이 감소되어 있었다. 식이 유도 비만 마우스의 복강으로 4 주간 NAD (1 mg/kg)를 주입하면 시상하부 NAD 부족을 극복할 뿐 아니라 비만 마우스에서 관찰되는 식이 섭취, 에너지 소비, 운동 활성 (locomotor activity)의 일중 주기 리듬의 둔화를 유의하게 호전시켰다. 이러한 결과는 NAD 의 보충이 시상하부 NAD 결핍과 연관된 대사 장애의 잠재적 치료 방법이 될 수 있음을 시사한다.

주요어: 시상하부, 비만, 에너지 항상성, 일중 주기, connexin